epl draft

Optimal Control of Superconducting N-level quantum systems

H. Jirari[1], F. W. J. Hekking[1] and O. Buisson[2]

[1] *LPMMC, C.N.R.S- Université Joseph Fourier, BP 166, 38042 Grenoble-cedex 9, France*
[2] *Institut Néel, C.N.R.S- Université Joseph Fourier, BP 166, 38042 Grenoble-cedex 9, France*

Abstract. - We consider a current-biased dc SQUID in the presence of an applied time-dependent bias current or magnetic flux. The phase dynamics of such a Josephson device is equivalent to that of a quantum particle trapped in a $1-$D anharmonic potential, subject to external time-dependent control fields, *i.e.* a driven multilevel quantum system. The problem of finding the required time-dependent control field that will steer the system from a given initial state to a desired final state at a specified final time is formulated in the framework of optimal control theory. Using the spectral filter technique, we show that the selected optimal field which induces a coherent population transfer between quantum states is represented by a carrier signal having a constant frequency but which is time-varied both in amplitude and phase. The sensitivity of the optimal solution to parameter perturbations is also addressed.

Introduction. – Superconducting circuits with Josephson junctions have received a lot of attention recently as promising candidates for scalable quantum bits [1, 2]. An example of such a circuit is the so-called phase qubit [3–5], which is based on a current-biased Josephson junction. The phase dynamics of this Josephson device is analogous to that of a quantum particle trapped in a $1-$D anharmonic potential. Preparation and control of the quantum states of the anharmonic well can be achieved by applying time-dependent current pulses to the system. The device can be used as a qubit when operated in the lowest two eigenstates of the anharmonic well.

The energy levels beyond the lowest two can be addressed as well. In particular, Rabi-like oscillations in the multilevel limit have been observed with a current-biased dc-SQUID [6]. In the context of quantum information processing, the coupling between the computational basis and the states of the noncomputational subspace results in adverse effects on quantum gate operations [7]. However, there is no need to restrict to only two energy levels. A generalization to qudits (*i.e.* systems with a single particle Hilbert space of dimension $d > 2$) has been proposed for quantum computation [8]. In this case, the quantum information is encoded in higher-dimensional Hilbert spaces.

Quantum computation requires a precise and complete control of quantum systems. The purpose of the present work is to apply optimal control theory to accurately transfer the populations of qudit states present in a current-biased dc-SQUID. The theory of optimal control is a well-developed field and finds numerous applications to the optimisation of nonlinear and highly complex dynamic systems [9]. In the quantum chemistry context, optimal control was originally proposed by Rabitz and co-workers [10] as a control scheme of reaction channels and was extensively used in various control experiments. Optimal control theory provides a systematic and flexible formalism that can be used in quantum computation to generate reliable and high precision quantum dynamics [11]. A very recent application deals with the optimization of a NOT-gate for phase qubits [12].

In the qudit case, population transfer can be realised via coherent transitions between quantum states interacting with the external control. In this letter we will use optimal control theory to demonstrate the possibility of a population transfer from the ground state to an arbitrary excited state of a quantum N-level system. In general, correlation and interference between the various pathways involved in the population transfer process cannot be ignored and lead to a possibly complicated dependence of the optimal control field on time which may be difficult to implement experimentally. We therefore restrict the frequency content of the control field using the spectral filter technique [13, 14]. This enables us to find optimized control fields that may be experimentally feasible.
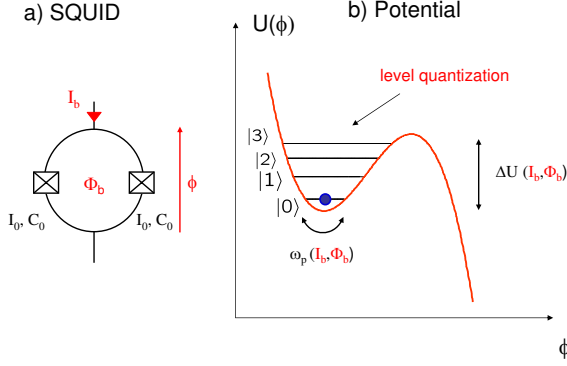
Fig. 1: (a) Current-biased DC SQUID. (b) Phase-dependent anharmonic potential with quantized levels.

Model. – We consider a dc-SQUID, biased with a current I_b, consisting of two Josephson tunnel junctions embedded in a superconducting loop, threaded by a flux Φ_b, see Fig. 1a. Each Josephson junction is characterized by its critical current I_0 and capacitance C_0. Using the mechanical analogy, it can be shown that the dynamics of the SQUID's phase ϕ is isomorphic to that of a fictitious particle of mass $m = 2C_0 \left(\Phi_0/2\pi\right)^2$ moving in one-dimensional anharmonic potential (harmonic oscillator with weak cubic perturbation) [6], see Fig. 1b. Here $\Phi_0 = h/2e$ denotes the flux quantum. Key parameters for the potential are the frequency of the bottom of the well ω_p and the barrier height ΔU. In the presence of a time-dependent external magnetic flux $\Phi_b(t)$, the quantum dynamics is described by the total Hamiltonian $\hat{H}_{\mathrm{tot}} = \hat{H}_\phi + \hat{H}_c$ where

$$\hat{H}_\phi = \frac{1}{2}\hbar\omega_p \left(\hat{P}^2 + \hat{X}^2\right) - \sigma\hbar\omega_p\hat{X}^3, \quad H_c = \hbar\omega_p\varepsilon(t)\hat{X}. \tag{1}$$

Here $\hat{P} = \left(1/\sqrt{m\hbar\omega_p}\right)P$ and $\hat{X} = \left(\sqrt{m\omega_p/\hbar}\right)\phi$ are the reduced momentum and position operators, respectively. The anharmonic dimensionless coupling σ can be tuned with the bias current; it is small compared to unity. The effect of a time-dependent external flux $\Phi_b(t)$ is included via the dimensionless function $\varepsilon(t) = \Phi_b(t)/\Phi_0$.

The theory described by the Hamiltonian $\hat{H}_\phi$, the basis Hilbert space of which is infinite, can be approximated by a theory described by an effective Hamiltonian (finite $N \times N$ matrix) $\hat{H}_{\mathrm{eff}} = \sum_{\mu,\nu=0}^{N-1}\langle\psi_\mu|\hat{H}_\phi|\psi_\mu\rangle|\psi_\mu\rangle\langle\psi_\nu|$ the basis of which is finite. Hamiltonian $\hat{H}_{\mathrm{eff}}$ reproduces only the low-energy physics of the system [15]. With the harmonic oscillator eigenfunctions $|\psi_\mu\rangle$ as the expansion basis, the matrix elements of $\hat{H}_\phi$ can be easily calculated. The eigenvalues E_n and wave functions $|n\rangle$ of the effective Hamiltonian can be obtained by diagonalizing $\hat{H}_{\mathrm{eff}}$ using a unitary transformation $\hat{H}_{\mathrm{eff}} = \mathcal{O}^\dagger\hat{H}_0\mathcal{O}$ where

$\hat{H}_0 = \mathrm{diag}(E_0, \dots, E_{N-1})$. Once the spectrum and wave functions are available, all physical information can also be obtained, especially the matrix elements of the control Hamiltonian $\hat{H}_c$ in Eq. (1). Within the exact diagonalisation of $\hat{H}_{\mathrm{eff}}$, the total Hamiltonian $\hat{H}_{\mathrm{tot}} = \hat{H}_\phi + \hat{H}_c$ is transformed into the driven N-level quantum system Hamiltonian whose form is $\hat{H} = \hat{H}_0 + \varepsilon(t)\hat{H}_I$ with

$$\hat{H}_0 = \sum_{n=0}^{N-1} E_n|n\rangle\langle n|; \quad \hat{H}_I = \hbar\omega_p\sum_{n,m=0}^{N-1} d_{n,m}|n\rangle\langle m| \tag{2}$$

where $\{|n\rangle : n = 0\dots N-1\}$ is a complete set of orthonormal eigenstates, *i.e.* the eigenvectors of $\hat{H}_{\mathrm{eff}}$ corresponding to the energies E_n. Here, the quantities $d_{n,m}$ are the transition dipole moments defined by $d_{n,m} = \langle n|\hat{X}|m\rangle = \sum_{\mu,\nu}\overline{C}_n^\mu C_m^\nu \int_{-\Lambda}^\Lambda dx\overline{\psi}_\mu(x)x\psi_\nu(x)$ where $C_n^\mu = \langle n|\psi_\mu\rangle$ and Λ is on the order of $10\sqrt{\hbar/m\omega_p}$. The off-diagonal elements of $\hat{H}_I$ induce transitions between energy eigenstates; the diagonal elements renormalize the energy eigenvalues, an effect known as the Stark shift.

Quantum optimal control problem. – Let time t be in the interval $[t_I = 0, t_F]$, for time t_F fixed. An arbitrary state of the system at time t can be represented by the density matrix ρ acting on $\mathbb{C}^N$, the Hilbert space of dimension N. The density matrix evolves according to the Liouville-von Neumann equation

$$i\hbar\dot{\rho} = \left[\hat{H}, \rho\right]; \quad \rho(0) = \rho_I \tag{3}$$

where ρ_I is the initial state of the system. We will use optimal control theory to design a control field $\varepsilon(t)$ which drives our system from an initial state ρ_I at time $t_I = 0$ to a desired target state ρ_F at specified final time t_F. The problem can be formulated in terms of a cost functional that also takes into account experimental constraints. Minimizing this cost functional leads to the desired physical target, thereby satisfying the constraints.

The question as to whether or not there exists a control that steers the system to a given goal is of crucial importance. For N-level quantum systems subject to a single control, this question has been addressed in [16, 17]. In the absence of dissipative effects, the answer is affirmative because the dynamical Lie group generated by $i\hat{H}_0$ and $i\hat{H}_I$ is isomorphic to the unitary group $U(N)$, which is compact. A target state ρ_F can be dynamically reached from ρ_I if there exists a unitary operator $\hat{U} \in U(N)$ such that $\rho_F = \hat{U}(t_F)\rho_I\hat{U}(t_F)\dagger$ [17]. Actually $U(t_F)$ represents the time evolution operator obeying itself the Schrödinger equation with the initial condition $\hat{U}(0) = \mathbb{1}$. The formal solution to the Schrödinger equation can be written as $\hat{U}(t_F) = \mathcal{T}\left\{\exp\left[-\frac{i}{\hbar}\int_0^{t_F} d\tau\,\hat{H}\right]\right\}$, where the symbol $\mathcal{T}$ denotes time ordering.

Pontryagin minimum principle. – Suppose the system is prepared at time $t_I = 0$ in the initial state

ρ_I. The objective is to compute an appropriate time-dependent control function $\varepsilon(t)$ steering the system from the initial state ρ_I into a target state ρ_F at fixed final time t_F. The corresponding cost functional may be written as

$$J[\varepsilon(t)] = \frac{1}{2}\|\rho(t_F) - \rho_F\|_F^2 + \frac{1}{2}\int_0^{t_F} \alpha(t)\varepsilon^2(t)\,dt \quad (4)$$

where $\|.\|_F$ is the Frobenius norm: $\|A\|_F^2 = \mathrm{Tr}A^\dagger A = \sum_{ij}|A_{ij}|^2$. Here, the first term represents the deviation between the state of the system at final time $\rho(t_F)$ and the target state ρ_F, whereas the second integral term penalizes the field fluency with a generally time-dependent weight α. We will illustrate the physical meaning of $\alpha(t)$ for a specific example below. Minimizing the first term (*i.e.* the error) is equivalent to maximizing the state transfer fidelity $F = \mathrm{Tr}\{\rho(t_F)\rho_F\}$. Our overall task is to find the control $\varepsilon(t)$ that minimizes $J[\varepsilon(t)]$ and satisfies both the dynamic constraint and the boundary condition (3). An optimal solution of this problem can be obtained using the first order optimality conditions in the form of the Pontryagin minimum principle (PMP) [18,19]. These conditions are formulated using a scalar pseudo Hamiltonian which may in the present case be cast in the form

$$\mathcal{H}(\rho,\varepsilon,\lambda) := \frac{1}{2}\alpha\,\varepsilon^2 + \mathrm{Tr}\left\{\frac{\lambda}{i\hbar}\left[\hat{H},\rho\right]\right\}, \quad (5)$$

where the adjoint state variable λ is an operator Lagrange multiplier introduced to implement the constraint (3). The PMP states that the necessary conditions of optimality for the control problem defined above are as follows:

$$\dot{\rho} = \partial_\lambda \mathcal{H} = \frac{1}{i\hbar}\left[\hat{H},\rho\right], \quad \hat{\rho}(0) = \rho_I; \quad (6)$$

$$\dot{\lambda} = -\partial_\rho \mathcal{H} = \frac{1}{i\hbar}\left[\hat{H},\lambda\right], \quad \lambda(t_F) = \rho(t_F) - \rho_F; \quad (7)$$

$$0 = \partial_\varepsilon \mathcal{H} = \alpha\varepsilon + \mathrm{Im}\,\mathrm{Tr}\left\{\frac{\lambda}{\hbar}\left[\hat{H}_\mathrm{I},\rho\right]\right\}. \quad (8)$$

The last condition is also equivalent to a vanishing gradient of the functional J with respect to the control ε,

$$\frac{\delta J}{\delta\varepsilon(t)} = \mathrm{Re}\int_0^{t_F}\partial_\varepsilon\mathcal{H}\left(\rho(t),\lambda(t),\varepsilon(t)\right)dt \quad (9)$$

$$= \int_0^{t_F}\left(\alpha(t)\varepsilon(t) + \mathrm{Im}\,\mathrm{Tr}\left\{\frac{\lambda(t)}{\hbar}\left[\hat{H}_\mathrm{I},\rho(t)\right]\right\}\right)dt. \quad (10)$$

Numerically, an iterative procedure based on successive linearization must be employed to find the optimal control. Here we will use a gradient-based method in order to find a solution to the system of the necessary conditions of optimality, Eqs. (6)-(8). More precisely, we have used the L-BFGS-B routine which is based on a bound constraint quasi-Newton method with BFGS update rule [20]. This routine is appropriate and efficient for solving constrained as well as unconstrained problems.

Population transfer. –   We now drive the system from the ground state $|0\rangle$ into one of the excited states $|n\rangle$, for $n = 1,2,3,\ldots$ as an illustrative example of the efficiency of the control field generated by the optimal control algorithm. Suppose the system is in state $\rho_I = |0\rangle\langle 0|$ at time $t = 0$. The objective is to force the system to state $\rho_F = |n\rangle\langle n|$ for given n at time t_F.

A variety of experimental constraints may be imposed in an optimal control problem in order to select control fields that are feasible from a practical point of view [14]. The purpose of the multiplier $\alpha(t)$ in the cost functional defined in Eq. (4) is to force the control field to approach zero at the initial and final time in accordance with the experiment. For this we use the shape function [18]

$$\alpha(t) = \alpha_0 + \alpha_1\left(\exp\left[-t/\tau\right] + \exp\left[-(t_F - t)/\tau\right]\right), \quad (11)$$

where the positive constants α_j are the penalty parameters and τ is a rise time. The role of α_0 is to penalize high control field values throughout the time interval $[0, t_F]$; α_1 together with the exponential terms enforces the field to be nearly zero at the boundaries of the interval $[0, t_F]$ while simultaneously turning on and off the field smoothly.

Because all the matrix elements of the interaction Hamiltonian H_I defined in Eq. (2) are different from zero the population transfer, for example from the ground state $|0\rangle$ to the excited state $|4\rangle$, will involve several pathways. The population transfer can be realized via a direct transition: $|0\rangle \longrightarrow |4\rangle$ or via indirect transitions: $|0\rangle \longrightarrow |1\rangle \longrightarrow |2\rangle \longrightarrow |3\rangle \longrightarrow |4\rangle$, $|0\rangle \longrightarrow |6\rangle \longrightarrow |4\rangle \ldots$ As a result, the time structure of the control field emerging from optimal control theory will generally be complicated, due to quantum mechanical interference between the pathways the field employs in the process $|0\rangle \longrightarrow |4\rangle$. The resulting control field is generally characterized by a frequency content that is not readily implemented experimentally. In order to reduce the control field complexity, we resort to the spectral filter technique. A convenient way to restrict the optimal field to a single desired frequency ω_0 is to filter the gradient by the formula [13,14],

$$\left.\frac{\delta J}{\delta\varepsilon(t)}\right|_\mathrm{filter} = \mathcal{F}^{-1}\left[g(\omega)\mathcal{F}\left[\frac{\delta J}{\delta\varepsilon(t)}\right]\right] \quad (12)$$

where

$$\mathcal{F}\left[\frac{\delta J}{\delta\varepsilon(t)}\right](\omega) = \frac{1}{\sqrt{2\pi}}\int_{-\infty}^{+\infty}\frac{\delta J}{\delta\varepsilon(t)}e^{-i\omega t}dt \quad (13)$$

is the Fourier transform of the gradient of the cost functional defined in Eq. (10) and

$$g(\omega) = e^{-\gamma(\omega-\omega_0)^2} + e^{-\gamma(\omega+\omega_0)^2} \quad (14)$$

is a Gaussian frequency filter centered around $\pm\omega_0$. Here γ is positive constant, large compared to the unity so that $g(\omega) = 0$ for $\omega \neq \pm\omega_0$ and $g(\omega) = 1$ for $\omega = \pm\omega_0$. During the optimization process, the control variable is updated

by a filtered gradient in each iteration. Thus, every spectral component in the control variable is eliminated except the components around $\omega = \pm\omega_0$. The resulting optimized control field has a simple intuitive interpretation.

The restriction of the spectrum to a single frequency $\omega_0 = (E_1 - E_0)/\hbar$ simplifies the time structure of the optimal control. Specifically, the time dependence of the control field can be interpreted as an input signal represented by a single oscillation of the form

$$\varepsilon_{\text{opt}}(t) = A(t)\cos\left[\omega_0 t + \varphi(t)\right] \qquad (15)$$

where the amplitude $A(t)$ and phase $\varphi(t)$ vary slowly with time compared to ω_0. The goal of complex demodulation is to extract the amplitude and phase as function of time [21]. First, the original signal $\varepsilon_{\text{opt}}(t)$ is multiplied by a complex modulation of frequency ω_0, yielding $f(t) = \varepsilon_{\text{opt}}(t)e^{-i\omega_0 t} = A(t)[e^{i\varphi(t)} + e^{-2i\omega_0 t - i\varphi(t)}]/2$. Passing the resulting signal $f(t)$ trough an ideal low-pass filter of cutoff frequency $\omega_c < \omega_0$ leads to $g(t) = A(t)e^{i\varphi(t)}/2 = \alpha(t) + i\beta(t)$. The time-dependent amplitude and phase can then be calculated as $A(t) = 2\sqrt{\alpha(t)^2 + \beta(t)^2}$ and $\varphi(t) = \arctan\left[\beta(t)/\alpha(t)\right]$, respectively.

Results. – We now illustrate the above concepts with the aid of some representative examples. Throughout this section, for the numerical simulations of population transfer from the ground state $|0\rangle$ to one of the excited states $|n\rangle$, we use the following nominal parameters, typical for experiments with current-biased SQUIDs [6] : anharmonicity $\sigma = 0.0325$; target time $t_F = 500/\omega_p$, chosen to be short enough to avoid substantial relaxation and decoherence phenomena; time step $\Delta t = 3.0 \times 10^{-2}/\omega_p$ corresponding to $M = 2^{14}$ as the number of mesh points; frequency filter $\omega_0 = (E_1 - E_0)/\hbar$; penalties factors $\alpha_0 = 10^{-1}$; $\alpha_1 = 10^2$ and rise time $\tau = 10^2/\omega_p$.

We start by considering the population transfer in a two-level system, $N = 2$. It is well-known that population transfer can be obtained within the rotating wave approximation (RWA) by applying a so-called π-pulse: a time-dependent signal of frequency $\omega_0 = E_1 - E_0$ (*i.e.* resonant with the level spacing) with duration equal to half of the so-called Rabi period. It is useful to study this simple example with the help of optimal control theory, as it enables one to compare to the known result for a π-pulse and hence test the numerical implementation; it also sheds some light on the functioning of the control procedure.

We first study the response of a two-level system to a π-pulse. The pulse is shown Fig. 2b, its complex demodulation is shown in panels (c) and (d). The response of the two-level system is obtained numerically and shown in Fig. 2a; we see that perfect population transfer is achieved. We subsequently use the π-pulse of Fig. 2b as a guess for an optimal control simulation, the results of which are shown in Fig. 3. It can be seen that the application of optimal control slightly modifies the original π-pulse. Specifically, the overall amplitude is smaller as a result of the
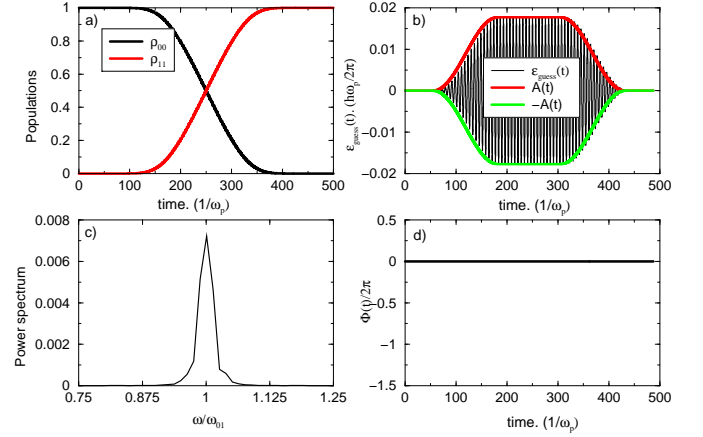

Fig. 2: Population transfer from the ground state $|0\rangle$ to the excited state $|1\rangle$, following a π-pulse. Panel (a) shows the numerically obtained evolution of populations, (b) and (c), respectively, show the π-pulse and its numerically obtained power spectrum. The amplitude of the pulse versus time is also shown in panel (b) while the numerically obtained time evolution of the phase is displayed in the panel (d).
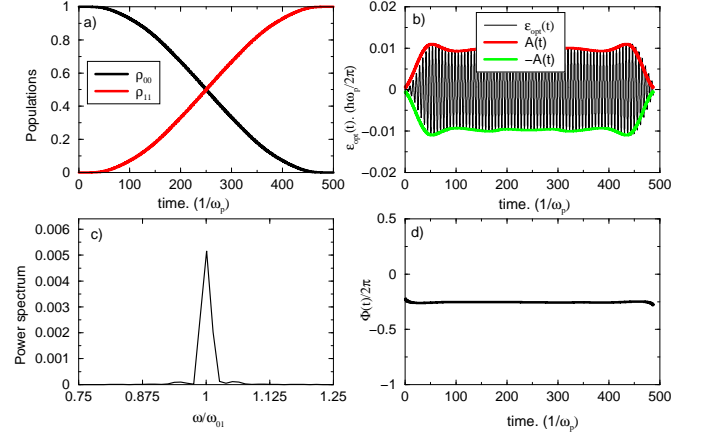

Fig. 3: Optimal control of population transfer from the ground state $|0\rangle$ to the excited state $|1\rangle$: (a) shows the evolution of populations, (b) and (c), respectively, show the selected control field and its power spectrum. The amplitude of the control field versus time is also shown in the panel (b) while the time evolution of the phase is displayed in the panel (d).

minimal amplitude constraint we imposed; the pulse duration has increased in order to conserve the total area of the envelope and hence the π nature of the pulse.

We next wish to implement a population transfer from the ground state $|0\rangle$ to the excited state $|1\rangle$ in a multilevel system with $N = 6$. As an initial guess we use the π-pulse of Fig. 2b. The response of the seven-level system to this guess is shown in Fig. 4a: the presence of the levels beyond $n = 1$ clearly leads to strong contamination effects that limit the efficiency of the transfer. We then use the initial guess as a starting point for an optimal control simulation; the resulting optimal pulse is shown in Fig. 5b, the result of the corresponding population transfer in panel (a). In order to avoid contamination, both the
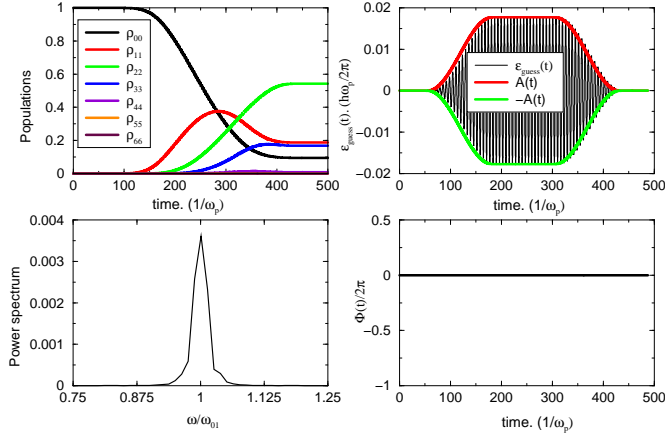
Fig. 4: Population transfer from the ground state $|0\rangle$ to the excited state $|1\rangle$ in a seven-level system, using a π-pulse; (a), (b), (c) and (d), as in the previous Figure.
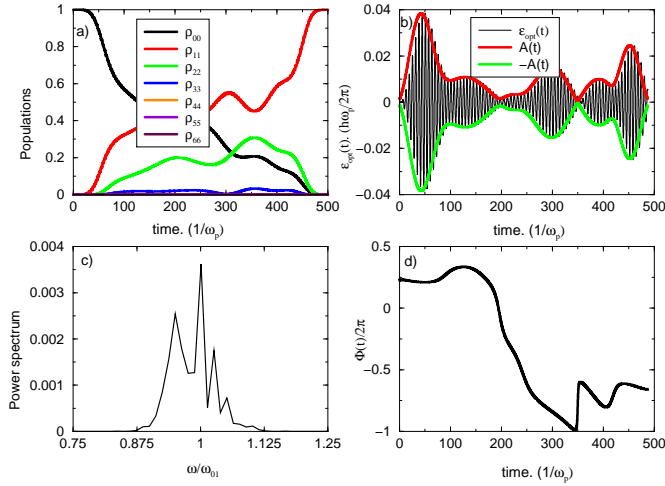

Fig. 6: Control of opulation transfer from the ground state $|0\rangle$ to the excited state $|4\rangle$ in a seven-level system; (a), (b), (c) and (d), as in the previous Figure.

Fig. 5: Control of population transfer from the ground state $|0\rangle$ to the excited state $|1\rangle$ in a seven-level system, using the π-pulse as a gues; (a), (b), (c) and (d), as in the previous Figure.

Fig. 7: Sensitivity of the population transfer to a small amplitude perturbation of the optimal control field.

pulse amplitude and its phase vary smoothly as a function of time, as shown in panels (c) and (d). We verified that a transfer from $|0\rangle$ to $|1\rangle$ can also be achieved in principle with a π-pulse similar to the one shown in Fig. 4b. However, the overall amplitude of the required pulse should be much smaller (by about a factor ten) in order to avoid non-resonant transitions to the higher levels. Accordingly the resulting duration would be ten times longer, thereby exceeding typical relaxation and decoherence times.

Finally, in Fig. 6, we show an optimal control simulation for the population transfer from the ground state $|0\rangle$ to the excited state $|4\rangle$. As can be seen by comparing panel (a) of Fig. 6 with that of Fig. 5, this transfer involves enhanced occupation during manipulation of the excited states of the system. We therefore expect transfers to higher states to be less robust against noise than transfers to low-lying excited states (see also the next Section).
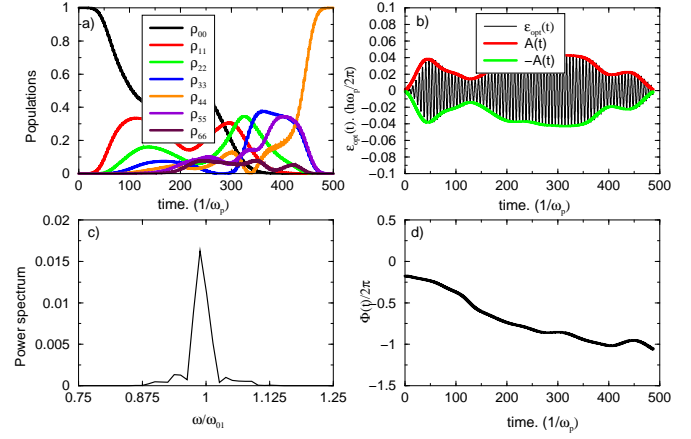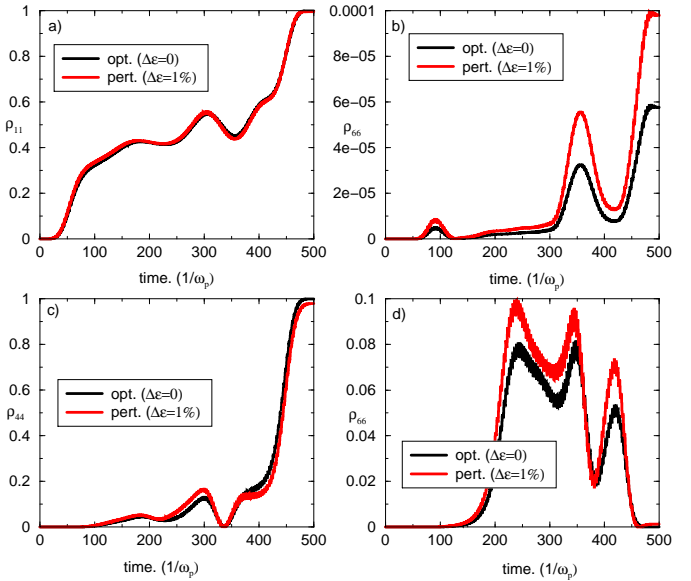
Sensitivity analysis. – In applications, the system parameters are usually not fixed but may be subject to perturbations and noises. For instance, the environment of the dc-SDUID induces time-dependent fluctuations of the bias current and flux. Because of the external perturbations, practical devices are not capable of operating precisely neither at the prescribed system parameters nor at the computed control field. Then, it is of great importance to know the sensitivity of the optimal solution with respect to perturbations of any of the system parameters. In this section, we shall only consider the influence of slow, adiabatic fluctuations. In the presence of this so-called adiabatic noise, the system parameters remain constant during a given manipulation but fluctuate during repetitive measurements needed to obtain quantum statistics.

In order to develop some feeling for the sensitivity of
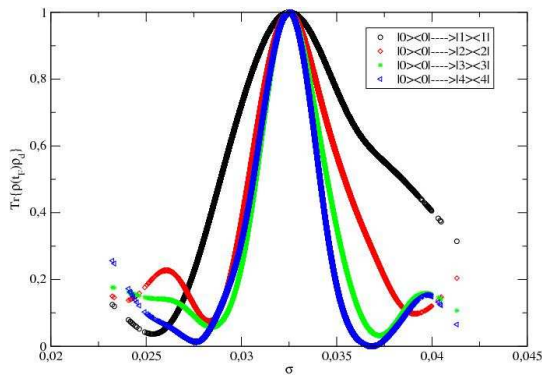
Fig. 8: Sensitivity of the population transfer fidelity to the random fluctuations of the anharmonic coupling.

the model system discussed here with respect to adiabatic noise, we show in Fig. 7 the effect of a small static amplitude fluctuation $\Delta\epsilon$ (of about 1%) with respect to the optimal amplitude on the result of the optimal control of a seven-level system when a population transfer from $|0\rangle$ to $|1\rangle$ is sought [panel (a) and (b)] or when a transfer from $|0\rangle$ to $|4\rangle$ is sought [panel (c) and (d)]. As is to be expected, the sensitivity to such a fluctuation is larger in the latter case, which involves more excited states during transfer.

We finally consider the effect of a slow variation of a system parameter during application of an optimal control pulse. Specifically, we assume variations of the anharmonic coupling σ to occur when the same optimal control sequence is repeated many times. Because the anharmonic coupling depends on the so-called working point, every random perturbation that changes the bias current or flux changes the parameter σ leading to uncertainties in the eigenvalues E_n and the transition dipole moments $d_{n,m}$ in Eq. (2). In Fig. 8 we show a plot of the state transfer fidelity F as a function of σ, calculated for a control field optimized for the case $\sigma = \overline{\sigma} = 0.0325$. The fidelity drops as σ deviates from $\overline{\sigma}$; we see again that it decreases faster as transitions to higher levels are considered. From this result we can calculate the average fidelity $\overline{F} = \frac{1}{M}\sum_{i=1}^{M} F_i = \frac{1}{M}\sum_{i=1}^{M} \text{Tr}\{\rho_i(t_F)\rho_d\}$, when the optimized control sequence is repeated M times, assuming σ to be a normally distributed random variable with a mean $\overline{\sigma} = 0.0325$ and a standard deviation $\Delta\sigma = \overline{\sigma}/16$. This choice corresponds to a typical experimental low-frequency noise present in phase qubits [4,5], yielding a Q-factor of about 1000. We find the following average state transfer fidelities: $\overline{F}_{|0\rangle\rightarrow|1\rangle} = 85\%$, $\overline{F}_{|0\rangle\rightarrow|2\rangle} = 73\%$, $\overline{F}_{|0\rangle\rightarrow|3\rangle} = 60\%$, and $\overline{F}_{|0\rangle\rightarrow|4\rangle} = 55\%$. If the low-frequency noise will be reduced only by a factor five (Q-factors ~ 5000), all the above fidelities remain larger than 95%.

Conclusion. – Using optimal control theory, we have studied the possibility of a population transfer from the ground state to an arbitrary excited state of a superconducting quantum N-level system. We have found that such state transfer can be obtained with good fidelity, us-ing optimized pulses which can be realized using existing microwave technology. We have considered the effects of low-frequency noise and found that it reduces the average state transfer fidelity. Using parameters describing actual phase qubits, we find a loss of fidelity of about 15 % for the transfer from level $|0\rangle$ to $|1\rangle$ up to 45 %, for a transfer from level $|0\rangle$ to $|4\rangle$. However, a substantial improvement of fidelity is possible by slightly decreasing the effects of low-frequency noise.

REFERENCES

[1] Yu. Makhlin, G. Schön, and S. Shnirman, *Rev. Mod. Phys. 73, 357-400 (2001).*

[2] G. Wendin and V. S. Shumeiko, *Superconducting quantum circuits, qubits and computing,cond-mat/0508729.*

[3] J. M. Martinis, S. Nam, J. Aumentado, and C. Urbina, *Phys. Rev. Lett.*, **89** (2002) 117901.

[4] M. Neeley *et al.*, *Nature Physics*, **4** (2008) 523.

[5] E. Hoskinson *et al.*, *arXiv: 0811.2174.*

[6] J. Claudon, F. Balestro, F. W. J. Hekking and O. Buisson, *Phys. Rev. Lett.*, **93** (2004) 187003.

[7] R. Fazio, G. M. Palma and J. Siewert, *Phys. Rev. Lett.*, **83** (1999) 5385.

[8] Marco Genovese and Paolo Traina, *Review on qudits production and their application to Quantum Communication and Studies on Local Realism, quant-ph/07111288.*

[9] Bryson A. E. and Ho Y. C, *Applied Optimal Control,* edited by Hemisphere, New York 1975.

[10] S. Shi and H. Rabitz, *J. Chem. Phys.*, **92** (1988) 3641988.

[11] M. Grace, C. Brif, H. Rabitz, I. A. Walmsley, R. L. Kosut and D. A. Lidar, *J. Phys. B: At. Mol. Opt. Phys.*, **40** (2007) S103.

[12] S.Safaei, S. Montangero, F.Taddei and R. Fazio, *arXiv: 0811.2174.*

[13] P. Gross, D. Neuhauser and H. Rabitz, *J. Chem. Phys.*, **96** (1991) 2834.

[14] J. Werschnik and E. K. U. Gross, *J. Phys. B: At. Mol. Opti. Phys.*, **40** (2007) R175.

[15] H. Jirari, H. Kröger, X.Q. Luo, and K. Moriarty, *Phys. Lett. A*, **258** (1999) 6.

[16] V. Ramakrishna, M. V. Salapaka, M. Dahleh, H. Rabitz and A. Pierce, *Phys. Rev. A.*, **51** (1995) 960.

[17] S. G. Schirmer, H. Fu and A. I. Solomon, *Phys. Rev. A.*, **63** (2001) 063410.

[18] H. Jirari and W. Pötz, *Phys. Rev. A*, **72** (2005) 013409; *Phys. Rev. A*, **74** (2006) 022306; *Euro. Phys. Lett.*, **77** (2007) 50005.

[19] A. K. Spörl, T. Schulte-Herbrüggen, S. J. Glaser, V. Bergholm, M. J. Storcz, J. Ferber, and F. K. Wilhelm, *Phys. Rev. A*, **75** (2007) 012302.

[20] *http://neos.mcs.anl.gov/neos/solvers/bco:L-BFGS-B/.*

[21] P. Bloomfield, *Fourier Analysis of time series: an introduction*, edited by Wiley, New York 1976, p. 147.